RAPID COMMUNICATIONS

PHYSICAL REVIEW C

NUCLEAR PHYSICS

THIRD SERIES, VOLUME 48, NUMBER 3 SEPTEMBER 1993

RAPID COMMUNICATIONS

The Rapid Communications section is intended for the accelerated publication of important new results. Manuscripts submitted to this section are given priority in handling in the editorial office and in production. A Rapid Communication in **Physical Review C** *may be no longer than five printed pages and must be accompanied by an abstract. Page proofs are sent to authors.*

Velocity correlations of intermediate mass fragments produced in central collisions of Au + Au at $E = 150A$ MeV

B. Kämpfer,[1,2] R. Kotte,[1] J. Mösner,[1] W. Neubert,[1] D. Wohlfarth,[1] J. P. Alard,[5] Z. Basrak,[13] N. Bastid,[5] I. M. Belayev,[9] Th. Blaich,[8] A. Buta,[3] R. Čaplar,[13] C. Cerruti,[11] N. Cindro,[13] J. P. Coffin,[11] P. Dupieux,[5] J. Erö,[4] Z. G. Fan,[6] P. Fintz,[11] Z. Fodor,[4] R. Freifelder,[6] L. Fraysse,[5] S. Frolov,[9] A. Gobbi,[6] Y. Grigorian,[10] G. Guillaume,[11] N. Herrmann,[7] K. D. Hildenbrand,[6] S. Hölbling,[13] A. Houari,[11] S. C. Jeong,[6] M. Jorio,[5] F. Jundt,[11] J. Kecskemeti,[4] P. Koncz,[4] Y. Korchagin,[9] M. Krämer,[6] C. Kuhn,[11] I. Legrand,[3] A. Lebedev,[9] C. Maguire,[11] V. Manko,[10] T. Matulewicz,[12] G. Mgebrishvili,[10] D. Moisa,[3] G. Montaru,[5] I. Montbel,[5] P. Morel,[5] D. Pelte,[7] M. Petrovici,[3] F. Rami,[11] W. Reisdorf,[6] A. Sadchikov,[10] D. Schüll,[6] Z. Seres,[4] B. Sikora,[12] V. Simion,[3] S. Smolyankin,[9] U. Sodan,[6] K. Teh,[6] R. Tezkratt,[11] M. Trzaska,[7] M. A. Vasiliev,[10] P. Wagner,[11] J. P. Wessels,[6] T. Wienold,[7] Z. Wilhelmi,[12] and A. L. Zhilin[9]

[1] *Forschungszentrum Rossendorf e.V., PF 51 01 19, 01314 Dresden, Germany*
[2] *Institut für Theoretische Physik (KAI e.V.), Technische Universität Dresden, Dresden, Germany*
[3] *Central Research Institute for Physics, Bucharest, Romania*
[4] *Institute for Physics and Nuclear Engineering, Budapest, Hungary*
[5] *Laboratoire de Physique Corpusculaire, Clermont-Ferrand, France*
[6] *Gesellschaft für Schwerionenforschung, Darmstadt, Germany*
[7] *Physikalisches Institut der Universität Heidelberg, Heidelberg, Germany*
[8] *Universität Mainz, Mainz, Germany*
[9] *Institute for Experimental and Theoretical Physics, Moscow, Russia*
[10] *Kurchatov Institute for Atomic Energy, Moscow, Russia*
[11] *Centre de Recherches Nucléaires and Université Louis Pasteur, Strasbourg, France*
[12] *Institute of Experimental Physics, Warsaw University, Warsaw, Poland*
[13] *Rudjer Bošković Institute Zagreb, Zagreb, Croatia*

(Received 27 May 1993)

Velocity correlations of intermediate mass fragments (IMFs), produced in central collisions of Au + Au at 150A MeV beam energy, are extracted from measurements with the FOPI (phase I) detector system at SIS in GSI Darmstadt. The IMF correlation function for semicentral events is found to be affected by the directed sideward flow. When rotating the events into a unique reaction plane an enhancement of correlations, resulting from event mixing effects, vanishes. Selecting violent collisions with a high degree of azimuthal symmetry the correlation function appears nearly independent of additional event or single particle gate conditions. The comparison of the data with a Coulomb dominated final-state interaction model points to an expanding and multifragmenting source with radius $R \sim 14$ fm.

PACS number(s): 25.70.Pq

Nuclear intensity interferometry supplies information on disassembling excited nuclear matter produced in heavy ion collisions. The space-time structure of the source which emits the reaction products can be explored by analyzing velocity correlations. This has been exploited for various kinds of particles produced in different reactions [1]. Intermediate mass or heavy fragments mainly undergo final-state Coulomb interaction, which prevents the proximity of such fragments in momentum space. Therefore, the appearence of small velocity differences of fragments is suppressed, in particular for small and/or short-living sources.

The analyses of velocity correlations of intermediate mass fragments (IMFs) with charges $Z \geq 3$ emitted in

asymmetric heavy ion reactions at beam energies $E < 100A$ MeV and in more symmetric reactions at beam energies of some tens A MeV point to considerable lifetimes of the IMF emitting source of the order of a few hundred fm/c [1–4]. This has been interpreted as an indication of a sequential decay of the primordial (compound-nucleus-like) system. On the other hand, theoretical models predict the dominance of a more instantaneous decay of the primordial fireball into IMFs and light particles in reactions of heavy nuclei at $E \simeq 100A$ MeV and larger [5,6]. Indeed, in a recent communication the authors report on multifragmentation time scales in central collisions of Ar + Au decreasing from $\sim$ 100 fm/c to $\sim$ 50 fm/c when varying the projectile energy from $35A$ MeV to $110A$ MeV [7]. A decrease of the space-time extent of the fragment emitter is also found in symmetric collisions Kr + Nb when increasing the beam energy from $35A$ MeV to $75A$ MeV [8]. Peripheral collisions of Xe + Cu at $50A$ MeV show a slower decay mode for fragment emission than central collisions [9]. The possibility of fast multifragmentation caused by high-energy light projectiles is a matter of debate [10,11].

In this work we analyze small-angle, small-relative-velocity correlations of IMFs. We present experimental data and a first interpretation of such two-body observables in central Au + Au collisions at $E = 150A$ MeV. In such heavy systems prominent flow effects appear at this energy. We use the Coulomb suppression of small relative velocities of neighboring IMFs to get information on the space-time structure of the source.

The data are taken by the highly granular, azimuthally symmetric "outer plastic wall" of the FOPI detector system at the heavy ion synchrotron SIS at GSI Darmstadt which is well suited for measuring velocity correlations. Details of the FOPI detector system can be found in Ref. [12]. The outer wall covers the polar angles of 7° to 30° with 512 scintillator strips in 8 radial sectors. Charge and velocity of the products are provided by ΔE-TOF (time of flight) measurement; in addition polar and azimuthal angles are determined. Ionization chambers in front of the outer plastic wall deliver the ΔE information and hence the charge Z of those fragments which are stopped inside the scintillator strips. (Double counting of one and the same particle caused by the small geometrical overlap of two strips or a nuclear reaction of the fragment in the detector material is mainly excluded in off-line analysis.) A helium-filled bag reduces energy losses and interactions of reaction products on their way between target and wall. The measured velocities are corrected for the energy loss in different media passed by the particles, including the target itself, which has a thickness of 200 mg/cm^2 (0.5% interaction probability). Energy thresholds of the detector system are given by $E_{\min} \simeq (15\text{–}50)A$ MeV for particles with charge Z = 1–15. The polar angle resolution is determined by the strip front height of 2.4 cm corresponding to $\Delta\Theta = 0.36°$. The position resolution σ(POS) along the scintillator strips is related to the mean-timing resolution σ(TOF)$\leq$ 0.20 ns by σ(POS)= $v_{\rm eff}\sigma$(TOF)$\leq$ 3 cm, with $v_{\rm eff}$ being the effective signal velocity along the strip. Relying on these values the relative-velocity resolution is estimated as $\sigma(v_{12}) \leq 0.005c$ for $Z_1 = Z_2 = 3$ fragments.

Events are classified by different binning procedures. Besides the IMF multiplicity we use the multiplicity of all charged particles seen in the outer plastic wall. Its distribution shows the typical flat plateau and a steep falloff at higher multiplicities. It is divided into five bins PM1–PM5. The highest-multiplicity bin PM5 starts at half the plateau value corresponding to an integrated cross section of 350 mb and a maximum impact parameter of 3.3 fm in sharp cutoff approximation [13]. The remaining multiplicity range is subdivided into four equally spaced intervals. The double selection of small values $D < 0.2$ (which defines the cut $D1$) of the transverse momentum directivity $D = |\sum_i \mathbf{p}_{\perp i}|/\sum_i |\mathbf{p}_{\perp i}|$ together with the high-multiplicity cut PM5 can be used to select high-centrality events, however, at the cost of a further reduction of the integrated cross section down to a value of 56 mb. Finally, the event-wise determined ratio of transverse-to-longitudinal sum energies $E_{\rm rat} = \sum_i (p_{\perp i}^2/M_i)/(\sum_i p_{\parallel i}^2/M_i)$ (assuming $M_i = 2Z_i m_N$) is found to be a much more effective centrality measure [14,15]. Already the single cut ERAT5 defined by $E_{\rm rat} > 0.74$ with about the same integrated cross section as in PM5 selects a pronounced IMF source at midrapidity, in a very similar way as the double cut PM5&D1 does on a much less statistical level. Supplementing information on one-body observables and event characterization can be found in Refs. [13–18].

The observed average IMF number per event $\langle M_{\rm IMF}\rangle$ is 1.5 (3.6) at charged particle multiplicity 17 (25) seen in the outer wall and rises continuously to 4.3 in PM5 where it seems to saturate. We have analyzed a total of about 8×10^5, 9×10^4, 2×10^4 IMF pairs in the event classes PM3–PM5, ERAT5, PM5&D1 and 7×10^4 pairs within an additional gate on the midrapidity region $y \sim y_{\rm cms} \pm \frac{1}{2}(y_{\rm proj} - y_{\rm cms})$ in PM5, respectively. Correlations of $Z_1 = Z_2 = 2$ clusters with prominent peaks at the known positions of the particle-unstable states ^{8}Be(g.s.), ^{8}Be(3.04 MeV), and ^{9}Be(2.43 MeV), which decay into two α particles, lend credibility to our data processing.

Let $Y_{12}(\mathbf{v}_1, \mathbf{v}_2)$ be the coincidence yield of IMF pairs with charges $Z_{1,2}$ and velocities $\mathbf{v}_{1,2}$. Then the two-particle correlation function is defined as [1]

$$1 + R_{12}(\mathbf{v}_1, \mathbf{v}_2) = \mathcal{N} \frac{\sum_{\rm events,pairs} Y_{12}(\mathbf{v}_1, \mathbf{v}_2)}{\sum_{\rm events,pairs} Y_{12,\rm mix}(\mathbf{v}_1, \mathbf{v}_2)}. \quad (1)$$

The sum runs over all events and pairs fulfilling certain selection criteria (see below). Event mixing, denoted by the subscript "mix," means to take IMF No. 1 and IMF No. 2 out of different events. We only mix events found within the same event class. $\mathcal{N}$ is a normalization factor fixed by the requirement to have the same number of true and mixed pairs. This normalization is as in Ref. [3]. The correlation function (1) is projected onto the hypersurface $v_{12} = |\mathbf{v}_{12}| = |\mathbf{v}_1 - \mathbf{v}_2|$. Besides the above-mentioned global event characteristics we use gate conditions on the pair rapidity $y = \frac{1}{2}(y_1 + y_2)$, on the pair velocity $V_{12} = |\mathbf{V}_{12}| = \frac{1}{2}|\mathbf{v}_1 + \mathbf{v}_2|$, or on the angle ξ between $\mathbf{v}_{12}$ and $\mathbf{V}_{12}$.

Mutual Coulomb repulsion within an IMF pair results in the scaled asymptotic relative velocity

$$v_{\rm red} \equiv \frac{v_{12}}{\sqrt{Z_1 + Z_2}} = \left(v_{\rm red,0}^2 + \frac{e^2}{m_N\, d_0} \right)^{1/2}, \qquad (2)$$

where the IMF mass numbers are $A_{1,2} = 2\,Z_{1,2}$, and the "initial" relative velocity and distance are $v_{12,0}$ ($v_{\rm red,0} = v_{12,0}/\sqrt{Z_1 + Z_2}$) and d_0 (e and m_N stand for elementary charge and nucleon mass). Please observe the charge independence of $v_{\rm red}$ as long as the Coulomb repulsion energy dominates. Indeed, when displaying $1 + R$ vs $v_{\rm red}$, instead of vs v_{12}, we find that different charge combinations result in rather similar curves [17]. This scaling, predicted in Ref. [19] and first verified experimentally in Ref. [20], is used in the following. It allows for systematical studies of the correlation functions even if rather restrictive event-selection criteria are applied. Otherwise, if only certain charge combinations were included the available statistics would be too low.

In Fig. 1 the yields of analyzed pairs are displayed as functions of the relative velocity and the relative azimuthal angle. In the relative-velocity yield [Fig. 1(a)] a slight shift towards higher values of $v_{\rm red}$ is observed when going from PM3 to PM5 to the more central ERAT5 bin. Selecting pairs from the PM5&D1 event class or pairs from the midrapidity region in PM5 events yields a similar distribution as found for ERAT5. The azimuthal distribution is sensitive to the event-selection criteria, too [see Fig. 1(b)]. It is discussed in more detail below. Figure 2 displays the experimental correlation function for all events in PM3–PM5. In the region $v_{\rm red} < 0.015c$ the mutual Coulomb repulsion causes the Coulomb suppression. It is located in a region of reduced statistics, as seen in a comparison with Fig. 1(a), where the maximum yield is at $v_{\rm red} \sim 0.06c$. In contrast to previous experiments [2,3], but in line with recent measurements [4,9], we find an enhancement of correlations at $v_{\rm red} \sim 0.025c$ (full squares in Fig. 2). When rotating all events into a unique reaction plane before event mixing the enhancement vanishes (see open squares). The reaction plane determination is performed with the transverse momentum analysis [21]. For the present setup the accuracy of the reconstruction of the reaction plane orientation is estimated as $\geq 30°$ on a 1σ confidence level [16]. Performing

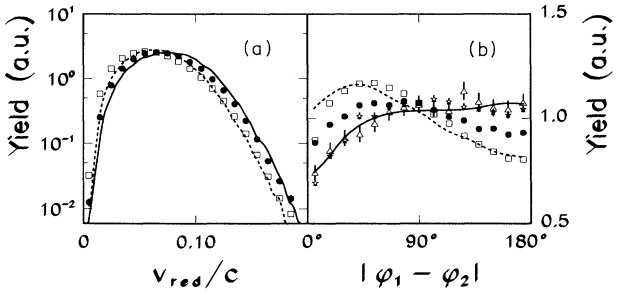

FIG. 1. The coincidence yield as function of reduced relative velocity (a) and azimuthal IMF pair distribution in the forward hemisphere as function of the relative angle (b). Squares, dots, triangles, and stars correspond to IMF pairs found under PM3–PM5, ERAT5, PM5&D1 cuts and midrapidity pairs in PM5 events, respectively (see text for explanation). The dashed and full lines display simulations with [parameter set (4)] and without [parameter set (3)] taking into account the directed flow.

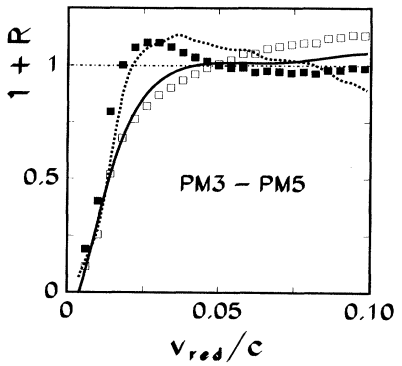

FIG. 2. The IMF correlation function for events in PM3–PM5 (full squares). The open squares are for the same events; however, they are rotated into a unique reaction plane before mixing. The full (dashed) line depicts the result of Coulomb trajectory simulations using parameter set (4) with (without) randomization of the reaction plane orientation $\mathbf{v}_\perp$.

this event rotation we believe to eliminate widely an unwanted effect of the sideward-directed flow of semicentral collisions (see below for further discussions).

In order to study the influence of the experimental setup on the correlation function we have performed Monte Carlo simulations with several event generators and the GEANT package [22]. As in the experimental data, we find an enhanced coincidence yield due to double countings at very small relative velocities ($v_{\rm red} < 0.005c$) mainly caused by secondary interactions in the scintillator strips. This disturbing yield, which is strongest for peripheral collisions, is reduced drastically by excluding, around a given hit, positions on neighboring strips within an azimuthal segment of $\Delta\phi = \pm\, 5°$. This procedure excludes also true hits. However, the simulation allows us to determine a lower relative-velocity limit above which the experimental correlation function is not systematically affected: For $v_{\rm red} > 0.006c$ the correlation function after filtering by the response of the apparatus (the finite angular, velocity and charge resolutions, the energy thresholds, and the exact geometry), suffers only minor distortions.

We have studied the dependence of the correlation function on various event characteristics and gate conditions and find the following results when rotating all events into a unique reaction plane before mixing [naturally, the event rotation does not have any influence on the mixing procedure if subgroups of azimuthally symmetric (i.e., low directivity) events are selected]: (i) There is no obvious dependence on IMF multiplicity observed in the outer wall acceptance. (ii) A slight dependence on the charged particle multiplicity of the Coulomb suppression, which is stronger for higher multiplicities, is attributed to the residual influence of sideward-directed flow in PM3–PM5 events after their rotation into a unique reaction plane. (Because of finite particle number effects the reaction plane determination is associated with a finite dispersion of typically 30°–40° for PM4 events.) (iii) Longitudinal and transversal correlation functions (i.e., pairs with $\xi = 0°$–$30°$ / $150°$–$180°$ and $\xi = 70°$–$110°$) do not differ significantly. However, they would show a strong splitting if the event rotation

into a unique reaction plane is not performed. (iv) The Coulomb suppression is stronger for central events selected by ERAT5 (see Fig. 3); no significant further shift of the correlation function in the considered interval is found if more restrictive $E_{\rm rat}$ conditions are applied or if PM5&D1 events are selected. (v) Pairs from the midrapidity region $y \sim y_{\rm cms} \pm \frac{1}{2}(y_{\rm proj} - y_{\rm cms})$ in PM5 events show the same correlation function as pairs from the ERAT5 or PM5&D1 events displayed in Fig. 3.

The error bars in Figs. 1–3, whenever shown, indicate statistical errors only. In the correlation function the errors are governed by those of the coincidence yield; the mixed yield is generated with an order of magnitude higher statistics.

In order to understand these experimental results and their global dependences we have performed different simulations, the results of which have been filtered through the detector acceptance. The present interpretation is based on calculations of N-body Coulomb trajectories of charged particles which are initially randomly and nonoverlappingly distributed in a sphere of radius R. Initially, the particles have a Maxwellian velocity distribution characterized by a temperature T. A collective radial expansion, with linear velocity profile $v(r) = (r/R)v_{\rm surf}$ (with $v_{\rm surf}$ as adjustable parameter), is superimposed on the random thermal initial motion. After Coulomb evolution the particle ensemble is boosted in longitudinal (to account for the cms motion) and randomly oriented in transverse direction (to mimic transverse directed flow of the foreward cms hemisphere particles which mainly are observed in the detector). Typically, 10^5 events ($\sim 10^6$ IMF pairs within the outer wall acceptance) have been generated for each parameter set.

In the following we show that for central collisions (characterized here by ERAT5) the parameters of the Coulomb simulation are widely constrained by experimental data: The experimental charge distribution is found to fall off exponentially $dN/dZ \sim \exp(-\alpha Z)$ for central events [23]. The slope parameter α and the averaged multiplicity $\langle M_{\rm IMF}\rangle \simeq 4$ of IMFs detected in the outer wall are used to fix the input charge and multiplicity distributions. Correcting for the limited phase space coverage of the present setup one gets $\alpha = 0.8$ and $\langle M_{\rm IMF}\rangle \simeq 12$ [16,23]. The radial expansion velocity parameter $v_{\rm surf}$ and the temperature parameter T we fix by the dependence of the averaged kinetic energy per nucleon $\langle E/A\rangle_{\rm cms}$ vs fragment mass A (assuming $A = 2Z$). Relying on the recent analysis of central events in ERAT5 [15,18] we use $\langle E/A\rangle_{\rm flow} = 12$ MeV and $T = 15$ MeV for the collective and randomized particle motions, respectively. The velocity of the radial expansion profile is related to the mean flow energy by $(E/A)_{\rm flow} = \frac{3}{10} m_N v_{\rm surf}^2$. Thus, the energy parameter translates into $v_{\rm surf} = 0.20c$. The transverse boost $v_\perp$ is the main variable for reproducing the enhanced correlations observed at $v_{\rm red} \sim 0.025c$. A systematic analysis of the directed flow [15,16] shows that on average not more than 1 MeV per nucleon resides in this collective transverse motion (whereas the available mean energy amounts to $37A$ MeV). This restricts the maximum transverse velocity to $v_\perp < 0.045c$. With the temperature and velocity parameters fixed in this way the experimental coincidence yield, displayed in Fig. 1(a), is well reproduced. In Fig. 3 the results of simulations with three different source radius parameters R are overlayed onto the experimental correlation functions. The normalization of the simulation curves is the same as for the experimental data. In order to find the optimum source radius (which is now the only remaining free parameter for fitting the Coulomb flank of the correlation function) we perform a χ^2 minimization of the simulated correlation function with respect to the experimental data for IMF pairs from central (ERAT5) events within the relative-velocity range $0.006c \le v_{\rm red} \le 0.05c$. The optimization leads to $R = 14 \pm 2$ fm where the error band corresponds to a deviation of ~ 1 from the minimum of χ^2 per degree of freedom (which amounts to 1.8). Finally, we find satisfying agreement with the data in Figs. 1–3 with a parameter set for central events (defined by ERAT5)

$$R = 14 \text{ fm}, T = 15 \text{ MeV}, v_{\rm surf} = 0.20c, \quad v_\parallel = v_{\rm cms} = 0.27c,\ v_\perp = 0, \tag{3}$$

and with another one for the PM3–PM5 events dominated by semicentral collisions (including randomly oriented sideward-directed flow and employing a somewhat higher longitudinal boost)

$$R = 14 \text{ fm}, T = 15 \text{ MeV}, v_{\rm surf} = 0.10c, \quad v_\parallel = 0.40c, v_\perp = 0.045c. \tag{4}$$

The parameters can be varied separately within an error range of $\sim 10\%$ without an obvious change of the curves in Figs. 1–3. An exception represents the random thermal motion parameter T which leads (as a consequence of the strong radial flow) only to minor distortions of the correlation function even when doubling the temperature. With the parameter set (4) we reproduce also the reduction of the enhancement of correlations at $v_{\rm red} \sim 0.025c$ when regarding the reaction plane orientation, here defined by $\mathbf{v}_\perp$ (see Fig. 2).

The experimental azimuthal IMF pair distribution in Fig. 1(b) is fairly well described, too. It evolves from a strongly asymmetric one for the mixture of central and semicentral events in PM3–PM5 to a more isotropic distribution for the central event selection PM5&D1 (trian-

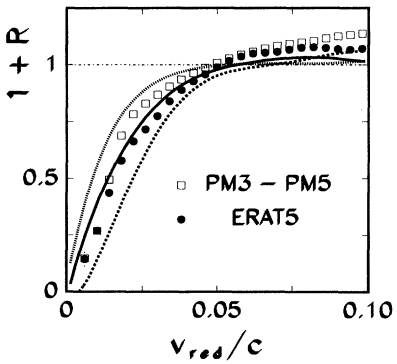

FIG. 3. The correlation function for IMF pairs from ERAT5 events (dots) and from the total ensemble of PM3–PM5 events (squares). The events are rotated into a unique reaction plane before mixing. The dashed, full, and dotted lines correspond to simulations with parameter set (3) but $R = 10$, 20, and 40 fm, respectively.

gles). From the simulation analysis the $\sim 25\%$ reduction in yield at small relative angles is found to be not only due to Coulomb suppression but also, though to a somewhat lesser extent, a result of momentum conservation and of proximity effects of the extended clusters within the source at the beginning of the radial expansion. The distribution of midrapidity IMF pairs in PM5 events [cf. stars in Fig. 1(b)] points to the selection of an approximately azimuthally isotropic IMF subgroup, too. The distribution of IMF pairs from ERAT5 events [see the dots in Fig. 1(b)] ranges in between the former ones, thus indicating that some sideward flow is still present in this event class [15,16]. In contrast to the IMF data shown here, the anisotropies of the corresponding relative-angle distributions of the light charged particles ($Z_{1,2} < 3$) are found to be much less pronounced. This is attributed to the lower nuclear charges and to the higher velocities of the random thermal motion of the light particles whereas the velocities of the heavier clusters are dominated by the flow [15,18].

It has to be noted that interpretations of the data without rotating the events into a unique reaction plane (see Fig. 2) within the Koonin-Pratt model [19] would point to significant source lifetimes [17]. The essential feature to be regarded indeed seems to be the directed IMF flow. Such collective effects are known to obscure correlation functions [24].

Our data interpretation indicates also a strong expansion effect. The extracted source radius of $R = 14$ fm is substantially larger than a $2A_{\mathrm{Au}}$ system at nuclear saturation density ρ_0. It corresponds to a freeze-out density of $\rho \simeq 0.2\rho_0$. Also this dilution is dominated by the radial flow: Without the flow (which, however, is needed to describe the dependence of the averaged energy per nucleon vs the fragment mass [15,18]) the $R = 10$ (20) fm correlation function would approximately coincide with the $R = 20$ (40) fm curve of Fig. 3 including the radial flow. In order to compensate for this strong shift a source radius, which is about two times smaller than the optimum one determined above, would be necessary.

One should have in mind that our simulations neglect dynamical correlations prior to the Coulomb evolution. Such primordial correlations may stem from the early fragment formation process, which is dealt with in different models [5,6,25–27]. Our two-body IMF observable data may serve as a crucial test of such models, in particular of dynamical event generators such as the QMD model [27].

In summary, we present small-relative-velocity correlations of IMFs produced in central collisions of Au + Au at 150A MeV. The data are compatible with a fast (instantaneous) multifragmentation picture of a radially expanding source created in central collisions. The importance of both radial and directed collective flow for the data interpretation is shown.

We are grateful to J. Pochodzalla and J. Randrup for supplying their simulation codes. Many discussions with H.W. Barz, D.H.E. Gross, H. Oeschler, J. Pochodzalla, and W. Trautmann are acknowledged. This work was supported by means of BMFT under Contracts No. 06 DR 105 and No. 06 DR 107.

[1] D.H. Boal, C.K. Gelbke, and B.K. Jennings, Rev. Mod. Phys. **62**, 553 (1990).
[2] Z. Chen *et al.*, Phys. Rev. C **36**, 2297 (1987); Y.D. Kim *et al.*, Phys. Rev. Lett. **67**, 14 (1991).
[3] R. Trockel *et al.*, Phys. Rev. Lett. **59**, 2844 (1987).
[4] T.C. Sangster, M. Begemann-Blaich, T. Blaich, H.C. Britt, A. Elmaani, N.N. Ajitanand, and M.N. Namboodiri, Phys. Rev. C **47**, 2457 (1993).
[5] D.H.E. Gross, Z. Phys. A **309**, 41 (1982); Phys. Rev. Lett. **68**, 146 (1986); Rep. Prog. Phys. **53**, 605 (1991).
[6] J.P. Bondorf, R. Donangelo, I.N. Mishustin, and H. Schulz, Nucl. Phys. **A444**, 460 (1985); J.P. Bondorf, R. Donangelo, H. Schulz, and K. Sneppen, Phys. Lett. **162B**, 30 (1985).
[7] D. Fox, R.T. de Souza, L. Phair, D.R. Bowman, N. Carlin, C.K. Gelbke, W.G. Gong, Y.D. Kim, M.A. Lisa, W.G. Lynch, G.F. Peaslee, M.B. Tsang, and F. Zhu, Phys. Rev. C **47**, R421 (1993).
[8] E. Bauge *et al.*, Phys. Rev. Lett. **70**, 3705 (1993).
[9] D.R. Bowman *et al.*, Phys. Rev. Lett. **70**, 3534 (1993).
[10] D.H.E. Gross, G. Klotz-Engmann, and H. Oeschler, Phys. Lett. B **224**, 29 (1989).
[11] J. Pochodzalla, Phys. Lett. B **232**, 41 (1989).
[12] A. Gobbi *et al.*, FOPI Collaboration, Nucl. Instrum. Methods **A324**, 156 (1993).
[13] J.P. Alard *et al.*, FOPI Collaboration, Phys. Rev. Lett. **69**, 889 (1992); cf. also GSI Scientific Report GSI-92-1, 1992, pp. 25–36.
[14] W. Reisdorf, FOPI Collaboration, in *Proceedings of the International Workshop, Hirschegg, 1992*, edited by H. Feldmeier (GSI, Darmstadt, 1992), p. 38.
[15] N. Herrmann, FOPI Collaboration, in Proceedings of the International Nuclear Physics Conference, Wiesbaden, Germany, 1992 [Nucl. Phys. **A553**, 739c (1993)].
[16] Th. Wienold, Ph.D. thesis, GSI Darmstadt, 1993.
[17] B. Kämpfer, R. Kotte, J. Mösner, W. Neubert, and D. Wohlfarth, FOPI Collaboration, in [14], p. 67.
[18] S.C. Jeong *et al.* (submitted to Phys. Rev. Lett).
[19] Y.D. Kim, R.T. de Souza, C.K. Gelbke, W.G. Gong, and S. Pratt, Phys. Rev. C **45**, 387 (1992).
[20] Y.D. Kim, R.T. de Souza, D.R. Bowman, N. Carlin, C.K. Gelbke, W.G. Gong, W.G. Lynch, L. Phair, M.B. Tsang, and F. Zhu, Phys. Rev. C **45**, 338 (1992).
[21] P. Danielewicz and G. Odyniec, Phys. Lett. **157B**, 3534 (1993).
[22] R. Brun, F. Bruyant, M. Maire, A.C. McPherson, and P. Zanarini, GEANT3, CERN Data Handling Division, DD/EE/84-1, 10.1987 (unpublished).
[23] C. Kuhn *et al.*, FOPI Collaboration, Phys. Rev. C **48**, 1232 (1993); J.P. Coffin, C. Kuhn, and J. Konopka, CRN Strasbourg Report CRN 92-50, 1992.
[24] S.E. Koonin, W. Bauer, and A. Schäfer, Phys. Rev. Lett. **62**, 1247 (1989).
[25] H.W. Barz, J.P. Bondorf, K. Sneppen, and H. Schulz, Phys. Lett. B **244**, 161 (1990).
[26] J. Hüfner, Phys. Rep. **125**, 129 (1985).
[27] A. Bohnet *et al.*, Phys. Rev. C **44**, 2111 (1991); G. Peilert *et al.*, *ibid.* **39**, 1402 (1989); J. Aichelin, Phys. Rep. **202**, 233 (1991).